

# An experimental approach for direct observation of the interaction of polyanions with sphingosine-containing giant vesicles

N.I. Hristova, M.I. Angelova<sup>1</sup>, I. Tsoneva\*

*Institute of Biophysics, Bulgarian Academy of Sciences, Acad. G. Bonchev Str., Bl.21, 1113 Sofia, Bulgaria*

Received 2 January 2001; received in revised form 10 April 2001; accepted 17 April 2001

## Abstract

A new approach for direct optical microscopy observation of polyanion interactions with bilayers of giant cationic liposomes (GUVs) was suggested. Polyanions as DNA, dextran sulfate (DS), heparin (H) and polyacrylic acids (PA) were locally delivered by a micropipette to a part of a giant unilamellar vesicle membrane. The phenomena were directly observed under optical microscope. GUVs, about 100  $\mu\text{m}$  in diameter, formed of phosphatidylcholines and up to 33 mol% of the natural bioactive cationic amphiphile sphingosine (Sph), were prepared by electroformation. The effects of water-soluble molecules with high negative linear charge density as dextran sulfate (DS), heparin (H) polyacrylic acids (PA) and adenosine-5'-triphosphoric acid (ATP) were compared with those of DNAs. The resulting membrane topology transformations were monitored in phase contrast, while the DNA distribution was followed in fluorescence. DNA-induced endocytosis-like membrane morphology transformation due to the DNA/lipid membrane local interactions was observed. The DS, H and PA induced membrane topology transformations similar to those of the DNAs, while ATP did not cause any detectable ones. The endocytosis mechanism involves the formation of ordered domains in the GUV membrane where some surface and charge asymmetries between the two membrane monolayers were created. The sizes of created polyanionic/cationic membrane domains depend on the form, length and elasticity of the adsorbed highly charged molecules. Endosome-including capacities of polyanionic molecules depend heavily on the high linear negative charge at a certain length.

An original method for direct studying of the DNA/membrane interactions in autoadaptable giant liposome system imitating biological membrane interactions was forwarded. The model observations could also help for understanding events associated with cationic liposome/DNA complex formation in gene transfer processes.

© 2002 Published by Elsevier Science B.V.

**Keywords:** DNA and polyanion interactions; Cationic GUV; Microinjection; Sphingosine; Endocytosis

## 1. Introduction

Experiments based on appropriate model systems can be very important for understanding the biophysical and biochemical nature of phenomena occurring when macromolecules (such as DNA of different sizes or other polyanion molecules) are brought into contact with model cationic lipid membranes. The DNA transport into cells has recently been thoroughly investigated.

Association of DNA with membranes and membrane/DNA complex formation plays a substantial role in bio-

logical processes as DNA replication and segregation [1–3]. Sphingosine (Sph), a breakdown product of cellular sphingomyelin, is a bioactive molecule, which regulates the transcription and replication processes, cell growth, differentiation and apoptosis by protein kinase C (PKC)-independent pathways [4–6].

Liposomes containing sphingosine have been systematically investigated [7–10] and have been used for DNA transfection with high efficiency and low toxicity [11]. When sphingosine is present in planar lipid bilayers, the adsorption of pDNA is enhanced and the electroporability of the bilayers is facilitated [12].

Liposomes containing synthetic cationic lipids are currently used as carriers of antisense oligonucleotides and plasmid DNA that regulate specific gene transfer [13–15]. On the other hand, the alteration in membrane morphology is frequently connected with changes in the cell functions,

\* Corresponding author. Tel.: +359-2-979-2622; fax: +359-2-971-2493.

E-mail addresses: itsoneva@obzor.bio21.bas.bg (I. Tsoneva), angelova@lpbc.jussieu.fr (M.I. Angelova).

<sup>1</sup> Present address: L.P.B.C., Univ. Pierre et Marie Curie (Univ. Paris VI), Case 138, 4 Place Jussieu, 75252 Paris Cedex 05, France.

e.g. apoptosis. Lately, the relationship between charges in lipid composition and membrane morphology has received a significant attention [16,17].

Considerable experimental and theoretical efforts have been focused on characterizing the structure of DNA/cationic liposome complexes [18–26] and on the transfection efficiencies [22]. Koltover et al. [22] have shown that the lipids, which are favorable for the formation of two-dimensional hexagonal  $H_{II}^C$  complexes, are more suitable in contrast to the lamellar  $L_{\alpha}^C$  structures for the DNA release into the cells.

The question is posed about the specificity of DNA/cationic GUVs interaction. Gruzdev et al. [27], using steady-state fluorescence anisotropy method, have observed that polyacrylic acid (PA) (which has no side-chain residues) forms the complex with lipid molecules in liposome suspension without shifting the phase transition temperature, as DNA and heparin (H) did. A mechanism of DNA release from cationic liposome/DNA complexes after their delivery into the cell has been suggested by Xu and Szoka [28]. Water-soluble polyanions with high linear charge density as dextran sulfate (DS) and  $H_{20000}$  have been successfully used to support this suggestion.

Despite the extensive investigations, the mechanism of DNA interaction with positively charged liposomes and the structure of the resulting complexes are still poorly understood. Surprisingly, all studies on DNA/liposome interactions have been performed so far “in bulk”, using liposome suspension. The addition of DNA to such suspensions leads to liposome aggregate formation [7,18,19,29–31]. No information about the effects of DNA interacting locally with a membrane, as a result of local and temporal delivery of DNA to a part of the membrane of an individual vesicle, was available before on the matter [26].

A new approach for direct optical microscopy visualisation has been developed and the interactions of individual vesicles with colloidal particles have been studied [32,33]. The effects of active substances microinjected locally to a part of the large unilamellar vesicle, prepared by electroformation method, have been evaluated [34–39].

In present work, the effects of DNA and charged anionic polymers as dextran sulfate, heparin and polyacrylic acids microinjected locally to GUVs containing sphingosine were visualised by an optical microscope. Adenosine-5'-triphosphoric acid (ATP) as a high charged molecule was also used.

## 2. Materials and methods

### 2.1. Chemicals

GUVs were prepared from 1,2-diphytanoyl-*sn*-glycero-3-phosphatidylcholine (DPhPC), 1-stearoyl-2-oleoyl-*sn*-glycero-3-phosphatidylcholine (SOPC), egg phosphatidylcholine (egg PC) and their mixtures with *D-erythro* sphingosine ( $Sph^+$ ) at phosphatidylcholine (PC) PC/ $Sph^+$

97:3, 93:7, 85:15, 75:25 and 67:33 mol%. (DPhPC, synthetic, Avanti Polar Lipids #850356; SOPC, synthetic, Sigma #P-9774;  $Sph^+$ , from bovine brain sphingomyelin, Sigma #S-6879.

The particular interactions of “short” [40] and “long” (26) DNAs with GUVs were studied. The “short” DNAs used were: (i) oligonucleotide, ss, DNA, 21b: 5'-CAACCA-TATCTACACAGGGTC-3', molecular weight (MW) =  $6.23 \times 10^3$  (kindly supplied by the Institute of Molecular Biology, BAS, Sofia). The “long” DNA used were: (i) super coil plasmid, pYep351, 5.6 kbp, MW =  $3.69 \times 10^6$ , contour length ( $L_{DNA}$ ) = 1.90  $\mu m$ , effective length ( $l_{DNA}$ )  $\sim 0.61 \mu m$  ( $L_{DNA} = N_{bp} \times 0.34 \text{ nm/bp}$ , and  $l_{DNA}$  is calculated according to Ref. [41]); (ii) three kinds of linear plasmid DNAs of different lengths: pUC19(EcoR), 2.7 kbp, MW =  $1.78 \times 10^6$ ,  $L_{DNA} = 0.92 \mu m$ ; pBR322, 4.3 kbp, MW =  $2.84 \times 10^6$ ,  $L_{DNA} = 1.46 \mu m$ ; psV3neo, 8 kbp, MW =  $5.28 \times 10^6$ ,  $L_{DNA} = 2.72 \mu m$ . The polyanionic species tested in order to elucidate the DNA specificity were: dextran sulfate, Na-salt, MW =  $5 \times 10^5$ , Serva; heparin MW =  $2 \times 10^4$ , Serva; polyacrylic acid of average MW =  $2 \times 10^3$  (PA<sub>2000</sub>) Aldrich, called “short PA”, and polyacrylic acid of average MW =  $2.5 \times 10^5$  (PA<sub>250000</sub>), Aldrich – 35 wt.% solution in water, called “long PA”; adenosine-5'-triphosphoric acid (ATP), disodium salt, MW =  $5.51 \times 10^2$ , Budapest, Hungary; Hoechst 33258 (Molecular Probes #H-1398, Ex/Em = 352/461).

Chemical structures of ATP, dextran sulfate, heparin and polyacrylic acid are shown in Fig. 1.

### 2.2. Preparation of liposomes and visualisation of membrane transformations

GUVs were formed by the liposome electroformation method following the experimental protocol described in Ref. [40]. The initial lipid deposit and the resulting GUVs become unstable for  $Sph^+$  concentrations higher than 33 mol%. The reason for the above effect could be the formation of charged clusters from sphingosine and their electrophoretic interaction with sinusoidal electric field at low frequency during the electroformation.

The DNA, DS, H, PA and ATP for local GUV microinjection were administered at a concentration of 0.01 mg/ml. DNA/GUV membrane interaction upon a single microinjection occurred under conditions of large excess of the lipid with respect to the DNA (about  $10^3$  lipid molecules/nucleotide for the targeted vesicle). DNAs were marked and visualised at Hoechst/nucleotide ratio 1:10. The Hoechst molecules in a water solution have three positive charges, tightly bound to the DNA helix, becoming fluorescent only after binding to DNA [42].

Microinjection was carried out by Eppendorf Transjector 5246. The microcapillary inner diameter for performing local microinjection to a GUV was 0.5–1  $\mu m$  in diameter. The injected volumes were of the order of a few picoliters ( $1 - 10 \times 10^{-12}$  l). The injection was performed from a distance

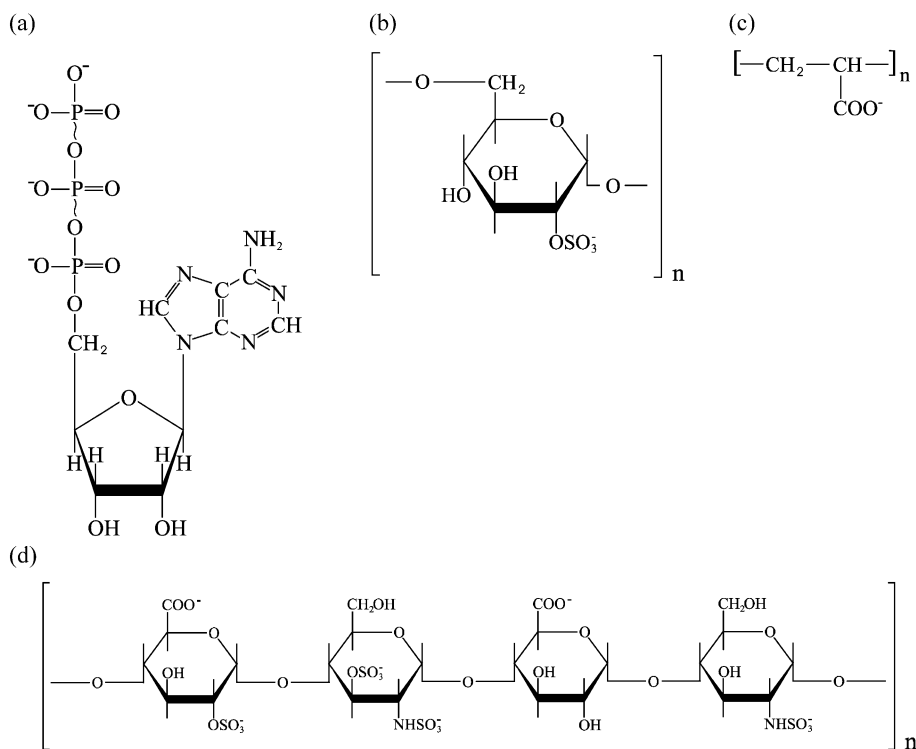


Fig. 1. Chemical structures of the polyanions used. (a) ATP: adenosine-5'-triphosphoric acid and segments of (b) DS: dextran sulfate, (c) PA: polyacrylic acids and (d) H: heparin.

of about 5  $\mu\text{m}$  from the GUV surface. The injected solution covers (visually and qualitatively determined) about 10% of the target GUV surface (for a GUV of about 100  $\mu\text{m}$  diameter). The present results are representative for at least five experiments of the same kind.

The kinetics of membrane morphology transformations after local microinjection of DNA, DS, H, PA and ATP to the GUV was followed in phase contrast. DNA (marked with Hoechst) fluorescence distribution was monitored by the Zeiss filter set 02 (Ex/Em = 365/>420 nm). The Zeiss Axiovert 135 microscope, equipped with Narishige MMN-1 plus MMO-22 micromanipulator, and Hamamatsu B/W Peltier chilled CCD camera (C5985-10) connected to an image recording and processing system were used.

### 3. Results

#### 3.1. "Short" DNA effects

DNA-induced endocytosis-like uptake due to "short" DNA/lipid membrane local interactions and complex formation was observed. The kinetics of the GUV morphology transformation was "explosive", i.e. endosome formation happened within 1–2 s after the "short" DNA delivery to the GUV membrane.

The image sequence shown in Fig. 2A presents the kinetics of membrane topology transformations of an initially quasi-spherical GUV (Fig. 2A-a), formed of DPhPC/Sph<sup>+</sup>

67:33 mol% as a result of the DNA 21b (marked with Hoechst dye) microinjection. The contact of the DNA molecules with the membrane upon the first injection destabilizes the latter, making the affected membrane part highly fluctuating. Eruption of vesicles towards the inner vesicle space (endosomes of about 5–10  $\mu\text{m}$  diameters) occurred for about 1 s (Fig. 2A-b). Fig. 2A-c illustrates the distribution of DNA fluorescence within the affected GUV. The DNA–Hoechst complex throughout the experiment (about 30 min) was stable and was visualised by a video camera.

A characteristic minimum concentration of Sph<sup>+</sup> ( $C_{\text{endo}}$ ) in the GUV membrane was necessary for the typical endocytic phenomenon to occur.  $C_{\text{endo}}$  depended on the type of the zwitterionic (PC) lipid used, being about 10 mol% for DPhPC/Sph<sup>+</sup> GUVs, and about 20 mol% for SOPC/Sph<sup>+</sup> or egg PC/Sph<sup>+</sup> GUVs. Below the  $C_{\text{endo}}$ , only lateral adhesions between neighboring vesicles were observed after DNA local microinjection.

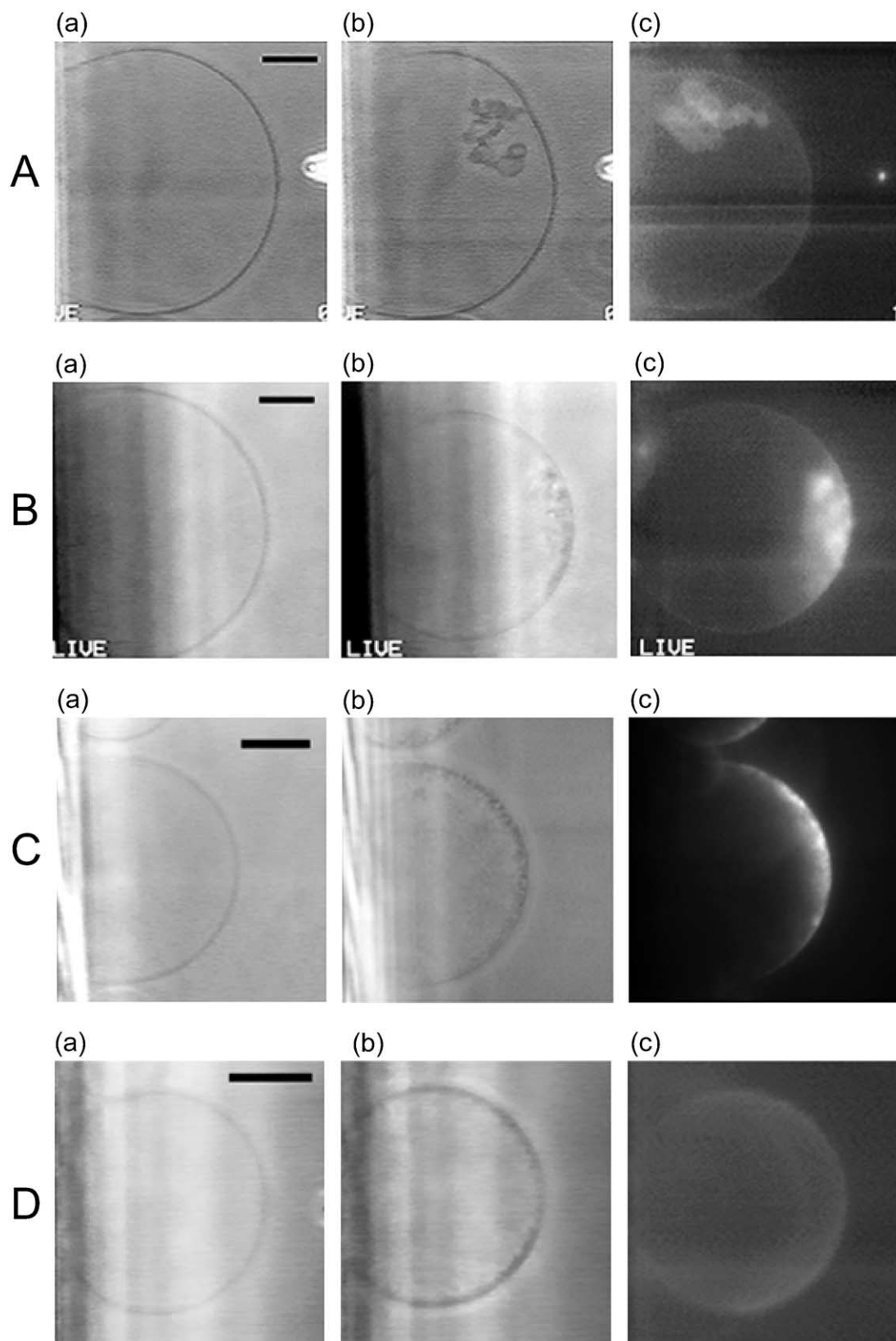
The capacity of DNA to induce endocytosis was reduced when it was fluorescently marked with Hoechst dye. Only strong irreversible adhesions between neighboring vesicles (but no endocytosis) were observed in the latter case (images not shown), probably due to the decreased (by the bound Hoechst species) charge density of the DNA.

#### 3.2. "Long" DNA effects

All "long" DNAs studied in this work induced endosome formation when injected to GUVs containing Sph<sup>+</sup>

above  $C_{\text{endo}}$  (established for the “short” DNA). However, the kinetics of the GUV morphology transformation was much slower than that of the “short” DNAs. The “long”

DNA-induced endosome formation took a few minutes after the injection. The characteristic endosome sizes were smaller; a particular population of dark, 1–2  $\mu\text{m}$  in diameter



particles appeared. These endosomes performed Brownian motion in the vicinity of the “mother GUV” membrane. It is difficult to say whether some connecting filaments exist. The shapes and capacities of the resulting endosomes to carry DNA were dependent on the particular “long” DNA molecular weight (Fig. 2B–D).

Fig. 2B presents the effects of pUC19(EcoR) (linear plasmid, 2.7 kbp—the “shortest” amongst the “long” DNAs tested) locally injected to a DPhPC/Sph<sup>+</sup> 67:33 mol% vesicle. Small, “dark” endosomes appeared in a couple of minutes (Fig. 2B-b). The marked DNA fluorescence was associated with the endosomes as well as with the “mother GUV” membrane (Fig. 2C-c).

When pYep351 (super coil plasmid 5.6 kbp) or pBR322 (linear plasmid, 4.3 kbp) was tested, only small, 1–2  $\mu\text{m}$  in diameter, “dark” endosomes appeared within 1–10 min (Fig. 2C-b). The marked DNA fluorescence was associated with these highly Brownian particles and was less spread over the “mother GUV” membrane (Fig. 2C-c). Typical images are shown in Fig. 2C for the case of pYep351 locally injected to a SOPC/Sph<sup>+</sup> 67:33 mol% vesicle.

Fig. 2D shows the effects of psV3neo (linear plasmid, 8 kbp—the “longest” DNA tested) locally injected to a DPhPC/Sph<sup>+</sup> 67:33 mol% vesicle. A peculiar result was obtained in this case: small, 1–2  $\mu\text{m}$  in diameter, “dark” endosomes appeared for about 10 min (Fig. 2D-b). However, the marked DNA fluorescence was associated only with the “mother” GUV membrane (Fig. 2D-c), and not with the endosomes. This suggests that the DNA in this case remains at the “mother” GUV membrane and was not transported with the induced endosomes in the GUV space.

### 3.3. Are these effects specific for DNA?

In order to clarify the specificity of DNA molecule for the observed phenomena, similar microinjection experiments with other polyanionic species were carried out. ATP solution was microinjected at different pressures, using a micropipette of inner diameter of 0.6  $\mu\text{m}$  (images not shown). No membrane topology transformations occurred after local microinjection of ATP at different pressures for longer times (up to a few seconds). There were some evidence for ATP becoming associated to the

GUV membrane (the membrane contour became darker). No changes of the vesicle diameter were detected.

Fig. 3A–D presents the membrane topology transformations after microinjection of dextran sulfate, heparin and polyacrylic acids. In all cases, endosomes were induced by the local microinjection of polyanion substances to the GUVs containing Sph<sup>+</sup> above  $C_{\text{endo}}$ . However, the particular kinetics, shapes and characteristic sizes of the induced endosomes were different.

Typical images after treatment with dextran sulfate are illustrated in Fig. 3A. Some black small spherical particles on the membrane surface immediately (for a second) after microinjection were observed (Fig. 3A-b). Formation of small endosomal vesicles (about 5  $\mu\text{m}$  in diameter) inside the liposome was registered, too. No bigger endosomes were observed. The black spherical particles are Brownian at the membrane and are stable for more than 10 min (Fig. 3A-c).

Heparin microinjected on the giant liposome induced a fast flow of membrane material into the giant vesicle interior (a second after microinjection). This membrane flow was not very well organized into the closed endosomes at the beginning (Fig. 3B-b). The kinetics of reorganisation of this membrane material was slow; some large closed endosomes were formed within 2–3 min (Fig. 3B-c).

In Fig. 3C, the image sequence presents the kinetics of membrane topology transformations as a result of the PA<sub>2000</sub> microinjection. The initially quasi-spherical, about 130  $\mu\text{m}$  in diameter GUV, made of DPhPC/Sph<sup>+</sup> 67:33 mol% was highly destabilized (membrane fluctuations of a few  $\mu\text{m}$  amplitude appeared) in the zone of the PA<sub>2000</sub> molecules delivery. Then (in a couple of seconds), a “sausage”-like membrane invagination started growing into the internal GUV space. The vesicle diameter decreased. This long and thin “sausage” (approximately 70  $\mu\text{m}$  in length and 5  $\mu\text{m}$  in diameter) was folded and pinched forming a few smaller multilamellar endosomes (Fig. 3C-b), which detached from the “mother” GUV membrane after 5–10 min, performing Brownian motion within the internal vesicle space (Fig. 3C-c).

Endosome (of 10- $\mu\text{m}$  sizes) formation occurred within 2–3 s after the PA<sub>250 000</sub> local delivery to a GUV membrane (Fig. 3D). The endosome number and characteristic sizes were smaller compared to those of the PA<sub>2000</sub> (for

Fig. 2. (A) Kinetics of membrane topology transformations of a GUV, made of DPhPC/Sph<sup>+</sup> 67:33 mol%, as a result of DNA 21b (marked with Hoechst dye) microinjection: (a) the initially quasi-spherical GUV; (b) eruptions of vesicles toward the inner vesicle space (endosomes about 5–10  $\mu\text{m}$  in diameter) occurred about 1 s after the DNA injection; (c) the distribution of marked DNA fluorescence within the affected. Bar=30  $\mu\text{m}$ . (Reproduced from Ref. [26] with permission from Elsevier Science). (B) Effects of pUC19(EcoR) (linear plasmid, 2.7 kbp) locally injected to a DPhPC/Sph<sup>+</sup> 67:33 mol% vesicle: (a) the initial GUV; (b) endosomes, (5  $\mu\text{m}$  in diameter), appeared within a few seconds after DNA injection, and small (1–2  $\mu\text{m}$  in diameter), “dark”, Brownian endosomes, appeared in a couple of minutes; (c) marked DNA fluorescence was associated with the endosomes as well as with the “mother” GUV membrane. Bar=20  $\mu\text{m}$ . (Reproduced from Ref. [26] with permission from Elsevier Science). (C) Effects of pYep351 (super coil plasmid, 5.6 kbp) locally injected to a SOPC/Sph<sup>+</sup> 67:33 mol% vesicle: (a) the initial GUV; (b) only small, 1–2  $\mu\text{m}$  in diameter, “dark”, Brownian endosomes appeared within 1–10 min; (c) marked DNA fluorescence was associated with these endosomes and was less spread over the “mother” GUV membrane. Bar=20  $\mu\text{m}$ . (Reproduced from Ref. [26] with permission from Elsevier Science). (D) Effects of psV3neo (linear plasmid, 8 kbp) locally injected to a DPhPC/Sph<sup>+</sup> 67:33 mol% vesicle: (a) the initial GUV; (b) small, 1–2  $\mu\text{m}$  in diameter, “dark”, Brownian endosomes appeared for about 10 min; (c) the marked DNA fluorescence was associated only with the “mother” GUV membrane and not with the endosomes. Bar=30  $\mu\text{m}$ . (Reproduced from Ref. [26] with permission from Elsevier Science).



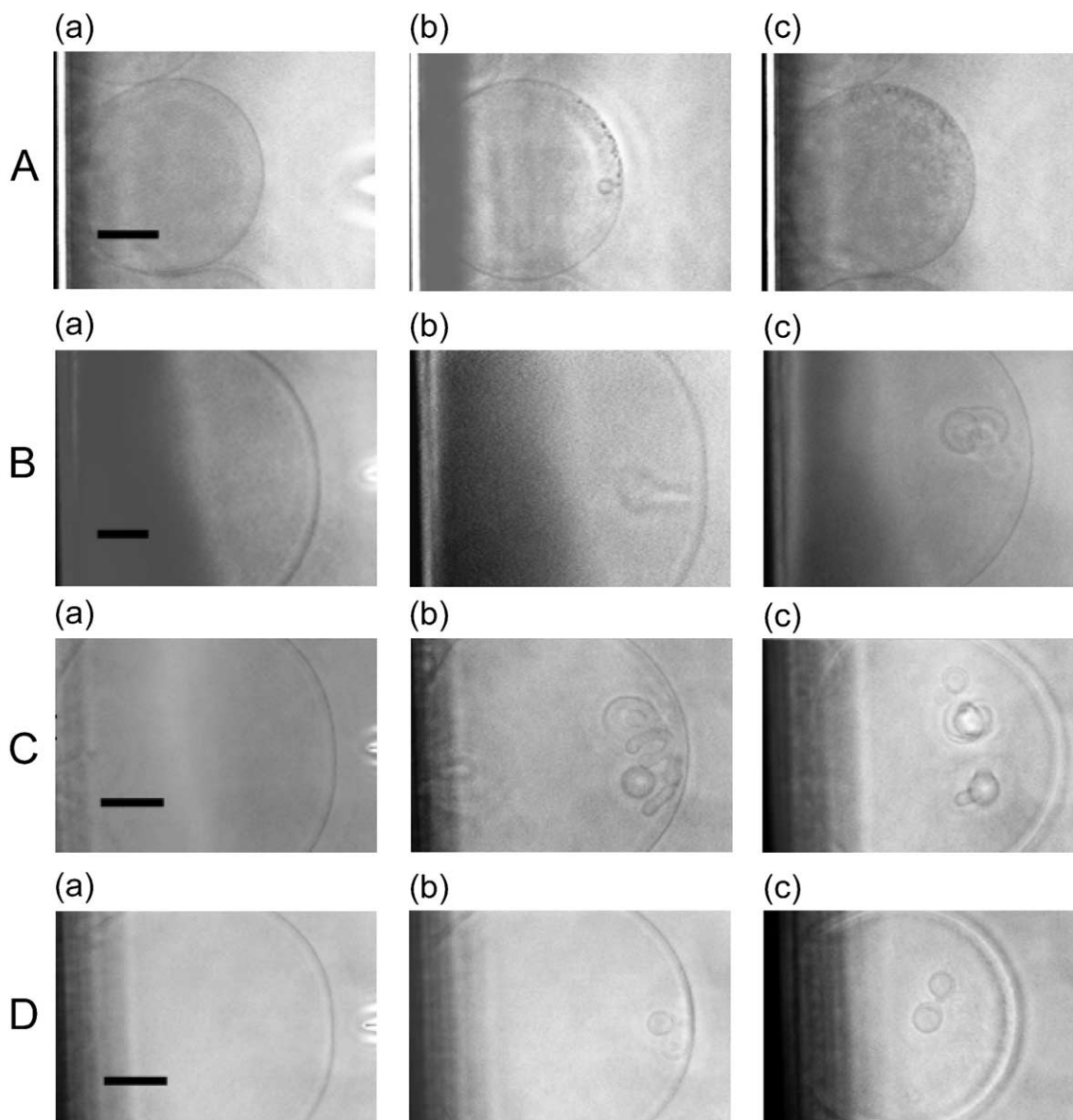


Fig. 3. (A) Effects of dextran sulfate, locally injected to a DPhPC/Sph<sup>+</sup> 67:33 mol% vesicle: (a) the initial GUV; (b) black, small vesicles on the membrane surface, formed for a second. Endosomes were small with a size of 3–5  $\mu\text{m}$  and (c) the black balls and endosomes moving on the surface after 10 min. Bar = 20  $\mu\text{m}$ . (B) Effects of heparin microinjected on the liposome from DPhPC/Sph<sup>+</sup> 67:33 mol%: (a) the initial GUV; (b) tunnel of membrane material into the liposomes after 1 s; (c) large endosomes were formed after 2–3 min. Bar = 20  $\mu\text{m}$ . (C) Effects of PA<sub>2000</sub> locally injected to a DPhPC/Sph<sup>+</sup> 67:33 mol% vesicle: (a) the initial GUV; (b) eruptions of vesicles towards the inner vesicle space (endosomes about 10–15  $\mu\text{m}$  in diameter) occurred about 1 s after the PA injection; (c) the evaluation of the formed endosomes, induced by PAA<sub>2000</sub>, 6 min after injection. Bar = 20  $\mu\text{m}$ . (D) Effects of PA<sub>250000</sub> locally injected to a DPhPC/Sph<sup>+</sup> 67:33 mol% vesicle: (a) the initial quasi-spherical GUV; (b) less in number, and small in sizes endosomes were formed after 1 min; (c) endosome migration, and “Brownian” endosomes appearing 6 min after injection. The diameter of the GUV was decreased almost twice. Bar = 20  $\mu\text{m}$ .

initial membrane tensions of the GUVs being similar). Small (about 2–3  $\mu\text{m}$  in diameter), “dark” endosomes appeared spreading along the “mother” GUV membrane 5–10 min later. The membrane contour became darker. The initial GUV diameter was decreased by 1/3 for 10 min (Fig. 3B-c).

Similarly to the case of DNAs, the injected PAs did not induce any membrane topology transformations when the concentration of Sph<sup>+</sup> in the GUVs was below  $C_{\text{endo}}$  (e.g. for DPhPC/Sph<sup>+</sup> 9:1 mol%). Unfortunately, we failed to

label fluorescently PA, H or D and to follow the distribution of polyanions in endosomes.

The experiments presented in this work were performed in distilled water at pH 5.5–6.0. The addition of 0.1  $\mu\text{g}$  of DNA, DS, H or PA to 1.2-ml distilled water did not cause significant changes in the pH. The presence of buffers or salts suppressed the GUV formation. The resulting vesicles were smaller in size, many of them being multilamellar and therefore not suitable for this kind of experiments. In all cases, the references mentioned in the introduction, as well

as the present results, led us to believe that the triggering interaction between the DNA and  $\text{Sph}^+/\text{PC}$  GUV membrane is of electrostatic origin.

## 4. Discussion

### 4.1. DNA lipid interaction

A comprehensive theoretical consideration of the molecular structure of polyionic/cationic liposome complexes was presented by May and Ben-Shaul [23] and Dan [20]. The interaction between adsorbing polyanions as DNA and the lipid heads changes the equilibrium lipid bilayer density, i.e. area per molecule, in the affected region of the outer lipid monolayer. The authors calculated a rise in the membrane-induced, attractive interactions between the adsorbed DNA molecules. This balanced the direct repulsive interactions between DNA molecules. As a result, DNA molecules adsorbed on membranes are predicted to form ordered domains characterized by finite spacing, which varies with the membrane characteristics and the solution Debye screening length.

Some possible mechanisms of the reorganisation of GUV membrane upon local interaction with different DNAs have been described in detail in earlier works [26,40].

Shortly, the possible mechanism of endosome formation is based on the idea of oligonucleotides DNA molecule encapsulation within an inverted micelle included in the lipid membrane (Fig. 2A). The outer monolayer decouples from the inner one and “rolls” up the DNA rod (DNA 21 bp could be considered as a rigid rod [40]), forming cylindrical defects resembling germs of inverted hexagonal structures.

According to Dan [20], the long DNA molecules adsorbed on membranes are predicted to form “ordered-DNAs super-domains” characterized by a finite regular DNA spacing. (N.B. Make the difference between lipid domains of different lipid composition, and “ordered-DNA super-domains”). Unfortunately, the author [20] does not consider the existence of a preferred “super-domain” size. Having this in mind and based on the present results, we suggest the following kinetics for the observed phenomenon: an important surface ( $S_{\text{ext}} < S_{\text{int}}$ ) and charge ( $\sigma_{\text{ext}}^+ < \sigma_{\text{int}}^+$ ) asymmetries between the two membrane monolayers are created upon the DNA/cationic membrane contact. These asymmetries are on the scale of the entire part of the GUV membrane, which contains “super-domains” and where DNAs (linear or supercoil with sizes less than 8 kbp) are adsorbed with some regular spacing between them. The mechanical properties of the vesicle membrane should have large lateral gradients due to the mosaic of super-domains. The created mechanical stresses relax by the formation of endosomes (with DNA), whose sizes are proportional to the size of the “super-domains” (Fig. 2B and C). It seems that a minimum “ordered-DNAs super-domain” size exists, which would bend to form a spherical endosome, corresponding to

a maximum DNA molecule length  $L_{\text{DNA,max}}$  (supercoil or linear).

The longest DNA tested (linear plasmid, 8 kbp) remains at the “mother” GUV membrane and is not transported with the induced endosomes (Fig. 2D). DNA molecules could not be ordered in DNA super domains with some regular distance between molecules if the adsorbed DNA molecules are larger than  $L_{\text{DNA,max}}$ . The membrane morphology transformations, in this case, could be explained by the so-called “archipelago effect” [43,44]. In brief, the effective lateral diffusion coefficient of individual lipids will decrease for longer DNA. The “archipelago effect” could inhibit the ability even of zwitterionic lipids trapped with the lipid/DNA domain to exchange with, and average over the bulk lipid population. In this case, the only-lipid domains will bend and form spherical endosomes (Fig. 2D).

The DNA anionic polymer added to the cationic amphiphile-containing lipid bilayer is able to laterally segregate cationic amphiphiles. Three types of reorganisation of other monolayer of liposomes containing sphingosine and the formation of endosome were suggested. Nevertheless, there are some similarities in all DNA tested, i.e. the creation of large membrane surface ( $S_{\text{ext}} < S_{\text{int}}$ ) and charge ( $\sigma_{\text{ext}}^+ < \sigma_{\text{int}}^+$ ) asymmetries, and thereby lateral gradients of the mechanical and electrical properties of the GUV membrane, resulting in membrane invaginations and endosome formations. The essential role for the creation of such asymmetries is the linear charge density of DNA.

### 4.2. Other polyanions effects

Dextran sulfate, heparin and polyacrylic acids induced formation of endosomes, probably based on similar interactions and mechanisms as the DNAs: important changes in surface ( $S_{\text{ext}} < S_{\text{int}}$ ) and charge ( $\sigma_{\text{ext}}^+ < \sigma_{\text{int}}^+$ ) asymmetries between the two membrane monolayers upon the polyanionic/cationic membrane contact (Fig. 3A–D). The kinetics of the changes in membrane topology in these cases is faster compared to the “long” tested DNAs. It should be pointed out that dextran sulfate exerted a somewhat particular effect compared to that of the other polyanions tested. The induced endosomes, if any, were much smaller. It might be correlated somehow with the “branched” structure of dextran sulfate polymer. All our results suggest that the linear charge density of polyelectrolytes is a critical factor for the electrostatic attractions to the charged surface and reorganisation of outer monolayer of giant liposomes. It seems that the endosome-inducing capacities of the polyanionic molecules depend heavily on the presence of high linear negative charge of a certain length. As already mentioned, the ATP molecule includes three phosphates and had a high negative charge linear density but very short length. The addition of ATP to the GUVs did not lead to any membrane topology changes.

The kinetics of endosome formation for “long” DNA was slower than that of other polyanions tested. This

suggests that upon the DNA electrostatic binding to the membrane surface, the adenosine bases could penetrate into the hydrophobic part of the lipid bilayer and reduce the endosome formation. Some evidence regarding the deep penetration of nucleotide bases into membrane interior has been presented in Refs. [27].

$C_{\text{endo}}$  was the same for DNAs and the other polyanions tested.  $C_{\text{endo}}$  depended on the fluidities of the lipids:  $C_{\text{endo}}$  was 10 mol% for DPhPC/Sph<sup>+</sup> GUVs (DPhPC is highly fluid at temperature  $T \geq -120$  °C) and about 20 mol% for SOPC/Sph<sup>+</sup> or egg PC/Sph<sup>+</sup>.

## 5. Conclusion

The model observations could help in understanding the events of the DNA association with biological membranes as well as the cationic liposome/DNA complexes formation in gene transfer processes.

A general approach (a method) for the direct study of the DNA/membrane interactions in an autoadaptable system (a system capable to change and adapt its local composition upon the interaction with an exogenic agent in order that the complex would be in equilibrium) is proposed. The method could easily be applied for evaluating the effects of a particular kind of DNA interacting locally with a (model or biological) membrane.

## Acknowledgements

This work was carried out in the French-Bulgarian Laboratory “Vesicles and Membranes” (Institute of Biophysics, BAS, Sofia) supported by the C.N.R.S. and the Bulg. Acad. of Sci. The contribution of the Bulgarian National Science Foundation (contract K707/97 to I.T.) is acknowledged as well. We thank Galya Staneva for re-organisation of the figures.

## References

- [1] W. Firshein, Role of the DNA/membrane complexes in prokaryotic DNA replication, *Annu. Rev. Microbiol.* 43 (1989) 89–120.
- [2] A.V. Aleschenko, V.A. Krasilnikov, P.Y. Boikov, Phospholipids as structural elements of nuclear matrix, *Dokl. Akad. nauk SSSR* 263 (1982) 730–733 (in Russian).
- [3] T. Kobayashi, R.E. Pagano, Lipid transport during mitosis, *J. Biol. Chem.* 264 (1989) 5966–5973.
- [4] Z. Hong, N.E. Buckley, K. Gibson, S. Spiegel, Sphingosine stimulate cellular proliferation via a protein kinase C independent pathway, *J. Biol. Chem.* 265 (1990) 71–81.
- [5] H. Zhang, N.N. Desai, J.M. Murphy, S. Spiegel, Increase in phosphatidic acid levels accompany sphingosine stimulated proliferation of Quiescent Swiss 3T3 cells, *J. Biol. Chem.* 265 (1990) 21309–21316.
- [6] C. Sakakura, E.A. Sweeney, T. Shirahama, S. Hakomori, Y. Igarashi, Suppression of Bcl-2 gene expression by sphingosine in the apoptosis of human leukemia HL-60 cells during phorbol ester-induced terminal differentiation, *FEBS Lett.* 379 (1996) 177–180.
- [7] P.K.J. Kinnunen, M. Rytömaa, A. Kõiv, J. Lehtonen, P. Mustonen, A. Aro, Sphingosine-mediated membrane association of DNA and its reversal by phosphatidic acid, *Chem. Phys. Lipids* 66 (1993) 75–85.
- [8] A. Kõiv, P. Mustonen, P.K.J. Kinnunen, Differential scanning calorimetry study on the binding of nucleic acids to dimyristoylphosphatidylcholine-sphingosine liposomes, *Chem. Phys. Lipids* 70 (1994) 1–10.
- [9] A. Kõiv, P.K.J. Kinnunen, Binding of DNA to liposomes containing different derivatives of sphingosine, *Chem. Phys. Lipids* 72 (1994) 77–86.
- [10] A. Kõiv, J. Palvino, P.K.J. Kinnunen, Evidence for ternary complex formation by histone H1, DNA and liposomes, *Biochemistry* 34 (1995) 8018–8027.
- [11] T. Paukku, S. Lauraeus, I. Huhtaniemi, P.K.J. Kinnunen, Novel cationic liposomes for DNA-transfection with high efficiency and low toxicity, *Chem. Phys. Lipids* 87 (1997) 23–29.
- [12] N.I. Hristova, I. Tsoneva, E. Neumann, Sphingosine-mediated electroporative DNA transfer through lipid bilayers, *FEBS Lett.* 415 (1997) 81–86.
- [13] P.L. Felgner, T.R. Gadek, M. Holm, R. Roman, H.W. Chan, M. Wenz, J.P. Nethrop, G.M. Ringold, M. Danielsen, Lipofectin: a highly efficient, lipid-mediated DNA-transfection procedure, *Proc. Natl. Acad. Sci. U. S. A.* 84 (1987) 7413–7417.
- [14] A. Singhal, L. Huang, *Gene, Therapeutics: Methods and Applications of Direct Gene Transfer*, Birkhäuser, Boston, 1994, p. 118.
- [15] O. Zelfhati, F.C. Szoka Jr., Liposomes as a carrier for intracellular delivery of antisense oligonucleotides: a real or magic bullet, *J. Control. Release* 41 (1996) 99–119.
- [16] P.K.J. Kinnunen, M.I. Angelova, J.M. Holopainen, Giant liposomes as models for lipid-mediated signaling in biomembranes, in: P.L. Luisi, P. Walde (Eds.), *Giant Vesicles*, Wiley, England, 1999, pp. 273–284.
- [17] J.M. Holopainen, M.I. Angelova, P.K.J. Kinnunen, Vectorial budding of vesicles by asymmetric enzymatic formation of ceramide in giant liposomes, *Biophys. J.* 78 (2000) 830–838.
- [18] H. Gershon, R. Ghirlando, S.B. Guttman, A. Minski, DNA mode of formation and structural features of DNA–cationic liposome complexes used for transformation, *Biochemistry* 32 (1993) 7143–7151.
- [19] B. Sternberg, Fr.L. Sorgi, L. Huang, New structures in complex formation between DNA and cationic liposomes visualized by freeze-fracture electron microscopy, *FEBS Lett.* 356 (1994) 361–366.
- [20] N. Dan, Formation of ordered domains in membranes-bound DNA, *Biophys. J.* 71 (1996) 1267–1272.
- [21] N. Dan, Multilamellar structures of DNA complexes with cationic liposomes, *Biophys. J.* 73 (1997) 1842–1846.
- [22] I. Koltover, T. Salditt, J.O. Raedler, C.R. Safinia, An inverted hexagonal phase of cationic liposome–DNA complexes related to DNA release and delivery, *Science* 281 (1998) 78–81.
- [23] S. May, A. Ben-Shaul, DNA–lipid complexes: stability of honeycomb-like and spaghetti-like structures, *Biophys. J.* 73 (1997) 2427–2440.
- [24] D. Harries, S. May, W. Gelbart, A. Ben-Shaul, Structure, stability, and thermodynamics of lamellar DNA–lipid complexes, *Biophys. J.* 75 (1998) 159–173.
- [25] P. Harvie, F.M.P. Wong, M.B. Bally, Characterization of lipid DNA interactions: I. Destabilization of bound lipids and DNA dissociation, *Biophys. J.* 7 (1998) 1040–1051.
- [26] M.I. Angelova, I. Tsoneva, Interaction of DNA with giant liposomes, *Chem. Phys. Lipids* 101 (1999) 123–137.
- [27] A.D. Gruzdev, V.V. Khramtsov, L.M. Weiner, V.G. Budker, Fluorescence polarization study of the interaction of biopolymers with liposomes, *FEBS Lett.* 137 (2) (1982) 227–230.
- [28] Y. Xu, F.C. Szoka Jr., Mechanism of DNA release from liposome/DNA complexes used in cell transfection, *Biochemistry* 35 (1996) 5616–5623.
- [29] I. Jääskeläinen, J. Mönkkönen, A. Urtti, Oligonucleotides–cationic liposome interactions: a physicochemical study, *Biochim. Biophys. Acta* 1195 (1994) 115–123.



- [30] J.O. Rädler, J. Koltover, T. Salditt, C.R. Safinya, Structure of DNA-cationic liposomes complexes: DNA intercalation in multilamellar membranes in distinct interhelical packing regimes, *Science* 275 (1997) 810–814.
- [31] K.W.C. Mok, P.R. Cullis, Structural and fusogenic properties of cationic liposomes in the presence of plasmid DNA, *Biophys. J.* 73 (1997) 2534–2545.
- [32] M.I. Angelova, B. Pouligny, G. Martinot-Lagarde, G. Grehan, G. Gouesbet, Stressing phospholipid membranes using mechanical effects of light, *Prog. Colloid & Polym. Sci.* 97 (1994) 293–297.
- [33] C. Dietrich, M.I. Angelova, B. Pouligny, Adhesion of latex spheres to giant phospholipid vesicles: statics and dynamics, *J. Phys., II Fr.* 7 (1997) 1651–1682.
- [34] R. Wick, M.I. Angelova, P. Walde, P.L. Luisi, Microinjection into giant vesicles and light microscopy investigation of enzyme mediated vesicle transformations, *Chem. Biol.* 3 (1996) 105–111.
- [35] M.I. Angelova, D.S. Dimitrov, Liposome electroformation, *Faraday Discuss. Chem. Soc.* 81 (1986) 303–311, disc: 345–349.
- [36] M.A. Guedeau-Boudeville, L. Jullien, J.M. di Meglio, Drug delivery: piercing vesicles by their adsorption onto a porous medium, *Proc. Natl. Acad. Sci. U. S. A.* 92 (1995) 9590–9592.
- [37] L. Mathivet, S. Cribier, Ph. Devaux, Shape change and physical properties of giant phospholipid vesicles prepared in the presence of an AC electric field, *Biophys. J.* 70 (1996) 1112–1121.
- [38] R. Wick, P.L. Luisi, Enzyme-containing liposomes can endogenously produce membrane-constructing lipids, *Chem. Biol.* 3 (1996) 277–285.
- [39] F.M. Menger, M.I. Angelova, Giant vesicles: imitating the cytological processes of cell membranes, *Acc. Chem. Res.* 31 (1998) 789–797.
- [40] M.I. Angelova, N. Hristova, I. Tsoneva, DNA induced endocytosis upon local microinjection to giant unilamellar cationic vesicles, *Eur. Biophys. J.* 28 (1999) 142–150.
- [41] M. Spassova, I. Tsoneva, A.G. Petrov, J.I. Petkova, E. Neumann, Dip patch clamp currents suggest electrodiffusive transport of the polyelectrolyte DNA through lipid bilayers, *Biophys. Chemist.* 52 (1994) 267–274.
- [42] F.G. Loontjens, P. Regenfuss, A. Zechel, L. Dumortier, R.M. Clegg, Binding characteristics of Hoechst 33258 with calf thymus DNA, poly[d(A-T)], and d(CCGGAATTCGG): multiple stoichiometries and determination of tight binding with a wide spectrum of site affinities, *Biochemistry* 29 (1990) 9029–9039.
- [43] M.J. Saxton, Lateral diffusion in an archipelago. Dependence of trace size, *Biophys. J.* 64 (1993) 1053–1062.
- [44] P. Mittrakos, P.M. Macdonald, DNA-induced lateral segregation of cationic amphiphiles in lipid bilayer membranes as detected via  $^2\text{H}$  NMR, *Biochemistry* 35 (1996) 16714–16722.